ISSN 1062-3604, Russian Journal of Developmental Biology, 2012, Vol. 43, No. 1, pp. 25–34. © Pleiades Publishing, Inc., 2012.
Original Russian Text © I.S. Vinogradova, O.V. Falaleev, 2012, published in Ontogenez, 2012, Vol. 43, No. 1, pp. 28–38.

PLANT DEVELOPMENTAL BIOLOGY

Formation of the Vascular System of Developing Bean (*Phaseolus limensis* L.) Seeds According to Nuclear Magnetic Resonance Microtomography

I. S. Vinogradova[a] and O. V. Falaleev[b]

[a] *Siberian State Technological University, pr. Mira 82, Krasnoyarsk, 660049 Russia*
e-mail: vis@akadem.ru

[b] *Kirenskii Institute of Physics, Krasnoyarsk Scientific Center, Siberian Branch, Russian Academy of Sciences, Akademgorodok, 660036 Russia*
e-mail: falaleev_ov@mail.ru

Received April 7, 2010; in final form, May 2, 2011

Abstract—^{1}H magnetic resonance microtomography imaging was applied to study vascular systems in developing bean (*Phaseolus limensis* L.) seeds. Using the gradient echo method, we recorded 2D tomographic sections in the sagittal and axial planes of the fruits sampled from a vegetating plant on days 10, 17, 24, and 31 after fertilization. Any vascular connection between the tissues of maternal plant (bean pod and seed coat) and the embryo were undetectable. The embryo has an autonomous branched network of procambial strands in the cotyledons, converging to the embryonic axis. The bean pods are covered with a network of vascular bundles; large vascular strands run along the dorsal and ventral sutures. The seed coat vascular bundles are formed in the process of seed ripening and are represented by a developed vascular system multiply branching in the middle part of the ground parenchyma at the stage of physiological maturity. They are connected with the source of assimilates via the lateral pod veins and a large vascular bundle, entering the seed below the hilum via the placenta. Assimilates enter the external part of the seed coat, which contains no vascular bundles, via the funiculus vascular bundles and hilum tissue.

Keywords: ^{1}H magnetic resonance microtomography, lima bean (*Phaseolus limensis*) seeds, seed development and ripening, vascular bundles, transport of assimilates.

DOI: 10.1134/S1062360412010079

INTRODUCTION

Nuclear magnetic resonance tomography imaging (MRI), widely applied in medicine (Rink, 2003), is actively introduced into biochemical and biophysical research (Callaghan, 1991; Koptyug and Sagdeev, 2002) as a new direction, NMR microtomography imaging, mainly using the signals of ^{1}H nuclei. This method is being constantly developed and improved and currently is widely used in plant research. An NMR microscope is able to detect free water in tissues and construct anatomic tomograms of tissues without destroying them.

Several reviews describe MRI application to plant studies (Chudek and Hunter, 1997; Ishida et al., 2000; Scheenen et al., 2000; Köckenberger, 2001; Ciobanu et al., 2003; Köckenberger et al., 2004; Scheenen et al., 2007; Van As et al., 2009). MRI was used to study seed swelling dynamics in soybean (Pietrzak et al., 2002), bean (Kikuchi et al., 2006), lupine (Garnczarska et al., 2007), tobacco (Manz et al., 2005), rice (Akemi et al., 2006), and other plants. These studies have succeeded in detecting the sites of water uptake in swollen seeds and determining its spatial distribution, which appeared nonuniform. The processes of natural drying during seed ripening have been studied in rice (Ishida et al., 2004), barley (Glidewell, 2006), and pea (Garnczarska et al., 2008) seeds.

One of the important problems in plant physiology is to study nutrient fluxes via vascular bundles. MRI has also contributed to solving this problem. The architecture of vascular bundles has been examined in strawberry (Goodman et al., 1992), raspberry (Williamson et al., 1994), apple (MacFall and Johnson, 1994), grape (Glidewell et al., 1997), and other fruits. Further elaboration of the MRI technique has brought forth the methods allowing the tissues of vascular bundles to be differentiated and the nutrient solution fluxes passing through them to be studied (Köckenberger et al., 1997; Verscht et al., 1998; Scheenen et al., 2000). In these works, they succeeded in distinguishing between the xylem and phloem in the images of plant stems and seedling hypocotyls as well as in calculating natural rates water fluxes and expenditures through them and in demonstrating an internal water circulation between phloem and xylem. Note that the

conductive system in stems is comparatively simple, being represented by parallel vascular bundles arranged in a concentric manner around the central part of the stem. The bundles are rather large; for example, the xylem in cucumber stem reaches a diameter of 0.35 mm. Their architecture and internal structure have been studied in detail with the help of light microscopy. However, little is known about the vascular system of plant seeds, and the available data have been obtained mainly by light microscopy of thin sections.

When studying water uptake into air-dry lima bean (*Phaseolus limensis* L.) seeds contacting water (Vinogradova and Falaleev, 2010a), we have found that water-saturated structures appear on tomograms in the cotyledons on completion of the first swelling stage. Analysis of the literature data (Tsinger, 1958), including the microtomography data (Garnczarska et al., 2008), has demonstrated that the discovered structures belong to vascular bundles. Further studies on grown lima bean (*P. limensis*) seeds at a physiologically mature stage (Vinogradova and Falaleev, 2010b) have demonstrated that individual fruit and seed tissues are well distinguishable in the tomogram as well as in the conductive tissues. Recording serial tomographic sections of beam seeds, we received images of vascular bundles of various architectures in the pod sections and sutures, seed coat, cotyledons, and embryonic axis. These results suggested setting the task of studying the bean seeds at different developmental stages and monitoring the formation of individual tissues and the vascular system by the MRI technique, which was the goal of this work. It was also of interest to compare the data obtained using two types of microscopy, MRI and light.

MATERIALS AND METHODS

Plant specimens

Lima bean plants were grown in a greenhouse from the seeds supplied by the limited liability company OOO Mistral Trading. The plants grew in a vertical direction reaching a height of over 2 m. The peduncles were multiflorous; however, almost all flowers fell down without setting. The first young fertilized buds set on only some of them in late August. This date was fixed to determine the time of seed ripening. The first experiments involved the seeds harvested 10 days after the indicated date; then seeds were harvested each week. In total, four seed batches (in triplicate) differing in their degree of maturation (on days 10, 17, 24, and 31 after setting) were examined. When recording the tomograms, the seeds remained inside the pod attached with funicula to the ventral suture.

MRI technique

NMR microtomography appeared in the mid-1980s. Characteristic of this method is a relatively low spatial resolution of approximately several tens and hundreds of micrometers, which is determined by a relatively low sensitivity and a spectral width of the NMR signal, which is rather large in the case of solids. A doubtless advantage of this method is the possibility to examine the internal structure and properties of objects, including optically nontransparent specimens, without destroying them, which is of paramount importance in biology and medicine. Another advantage is the possibility to obtain information along any direction. The overwhelming majority of studies have been performed using ^{1}H NMR signals. MRI is a powerful tool for studying water in living systems. MRI technique is detailed in several monographs (Farrar and Becker, 1971; Morris, 1986; Pfeffer and Gerasimowicz, 1989; Callaghan, 1991; Hausser and Kalbitzer, 1991; Blümich and Kuhn, 1992).

In NMR, the signal resonance frequency (for example, from protons of water) is usually directly proportional to the value of external magnetic field applied to the specimen, which is set maximally uniform in the case of a high-resolution NMR spectroscopy. If a studied specimen is exposed to a nonuniform field linearly changing along a selected direction in space, i.e., when creating a field gradient, as was proposed by Lauterbur (1973), then the resonance frequency will change proportionally to the coordinate in the specified direction. To assay a 3D object, it is necessary to create a field gradient in three mutually perpendicular directions. This method makes it possible to obtain something like anatomical sections of a 3D body. For this purpose, it is sufficient when exciting the specimen to create a gradient of external field in the direction perpendicular to the plane of the necessary section. Correspondingly, at a specified "excitation" frequency of atomic nuclei, only the nuclei for which this is a resonance frequency, i.e., the nuclei located in a certain plane of body section, will be excited. This method provides for recoding an image of the overall section with the depth and orientation specified by the operator. The image is constructed by a computer via two-dimensional Fourier transform. Usually, up to 30 sections and more can be concurrently recorded.

A magnetic field is created by a superconducting coil using liquid nitrogen and liquid helium in the cooling system. The atomic nuclei are excited using a coil powered with a radiofrequency (RF) generator; in this process, different parts of the specimen are exposed to magnetic fields of different strengths and give the NMR signal from the same spatial coordinate. Use of three mutually perpendicular field gradients makes it possible to study the dependence of NMR signal on two or three spatial coordinates, thereby giving two- and three-dimensional images, respectively.

Our tomographic experiment was conducted at the Krasnoyarsk Joint Access Regional Center (Siberian Branch, Russian Academy of Sciences) using a Bruker (Germany) microtomograph, comprising the follow-

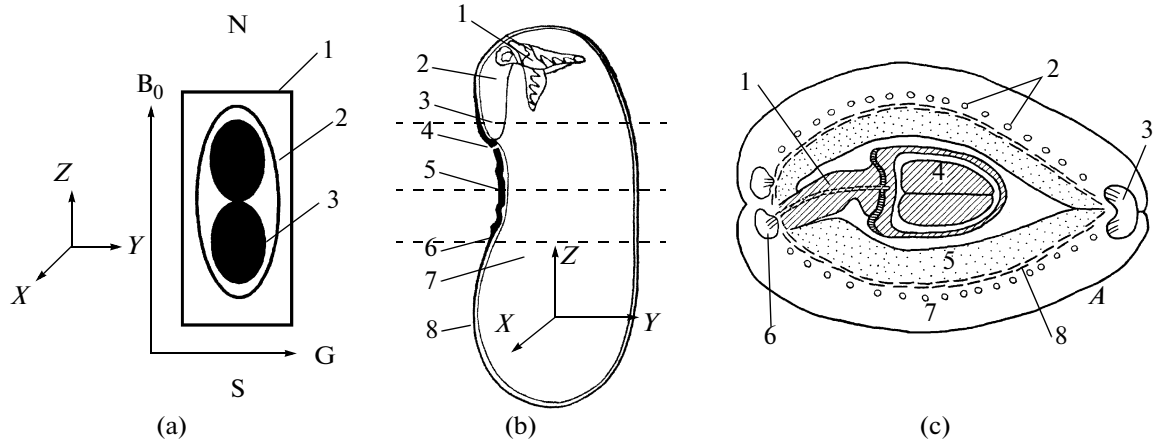

Fig. 1. (a) Location of lima bean fruit in radiofrequency circuit relative to the static magnetic field B_0; *X*, *Y*, and *Z* are the axes of laboratory system of coordinates; the magnetic field gradient (G) is created along the Y axis: (1) specimen holder, (2) bean fruit; and (3) bean seed. (b) and (c) Scheme of bean seed. (b) Longitudinal section: (1) budlet; (2) hypocotyl; (3) radicle; (4) micropile; (5) seed hilum; (6) lens; (7) cotyledons; and (8) seed coat. Dashed lines denote the planes of tomographic cross-sections: upper, through the radicle of embryonic axis (Fig. 2d); middle, through the hilum (Fig. 2e); and lower, below the hilum at the entrance of a vascular bundle to seed coat (Fig. 2f). (c) Cross-section of the fruit at the level of embryonic cotyledons: (1) funiculus; (2) vascular bundles of the pod; (3) median carpel bundle; (4) cotyledon; (5) inner parenchyma; (6) lateral carpel bundle; (7) outer parenchyma; and (8) sclerenchyma (reproduced from Esau, 1980).

ing main units: a US 200/85 vertical superconducting-coil electromagnet for 4.7 T, DPX 200 console, GRE AT 40 console, PH 200 WB (MINI 0.5 and MICRO 2.5) sensors, LINUX (KDE 3.5) operating system, and Para Vision 4.0 software. The maximal specimen size is limited by the inner diameter of the RF coil, amounting to 37 mm; the range of stabilized temperature was ±70°C. Tomographic images were reconstructed using a 512 × 512 px image sensor and a field of view of 1.5 cm for small objects to 3.0 cm for large ones. A gradient echo technique (Gyngell, 1988) was used in this work. The pulse repetition period (T_R) was 300–400 ms; echo time (T_E) was 4 ms; and the angular deflection of magnetization by the excitation RF pulse was 30 degrees.

Individual bean fruits were placed in an RF circuit of spectrometer as is shown in Fig. 1a. The lima bean seeds are rather large, and one pod contains one to three seeds. Pods with two seeds were used in the experiment; they were placed vertically in the sensor. The sections were recorded for only one seed. The pods containing seeds of approximately the same size were selected. The measurements were performed at a room temperature (20–23°C). The tomographic sections were recorded in two mutually perpendicular planes: sagittal, perpendicular to the *X* axis and parallel to the embryonic axis (Fig. 1b), hereinafter refereed to as longitudinal, and axial, perpendicular to the embryonic axis (perpendicular to the *Z* axis in Fig. 1b), hereinafter referred to as cross-sections. The section thickness is shown in the corresponding figures. The number of sections was 25 to 36. A large number of sections is determined by the fact that the vascular system in the pod, its ventral and dorsal sutures, seed coat, cotyledons, and seed embryonic axis has different architectures; correspondingly, the patterns of bundles are rapidly changing. Therefore, we had to make rather thin sections, decreasing the signal-to-noise ratio, especially in the case of early developmental stages. To increase the signal-to-noise ratio, we used a 40-fold accumulation. All this increased the time for tomogram recording (4 h), although one of the advantages of the gradient echo technique consists in short measurement time at the expense of small angular deflection of magnetization.

RESULTS

Maturation of the beam seeds takes 53–56 days from the beginning of flowering (Öpik, 1968). The seed development that follows fertilization is usually divided into three phases (Weber et al., 2005), which correspond to stages X–XII of organogenesis (*Fiziologiya...*, 1970). Our data have been obtained for phases X and XI.

We have obtained a large number of MRI sections for each specimen, and they all cannot be demonstrated in a single paper; therefore, we selected the sections crossing the bean pod wall, seed coat, funiculus, embryonic axis, and cotyledons in order to reflect the architecture of vascular bundles and the routes of nutrient inflow from the maternal pant to development seed.

Figure 2 shows tomographic cross-sections; the day after fertilization is indicated under each image; arrows show the scale (5 mm). Figures 2a–2d show the sections in the plane passing through the embryonic axis. To demonstrate the main routes of water and

nutrient uptake by the developing seed, the section passing through the center of the seed, hilum tissue, and funiculus are shown (Fig. 2e); in Fig. 2f, the section passes below the hilum at the entrance site of a large vascular bundle. The sections are denoted with dashed lines in Fig. 1b. To identify the bean tissues, we reproduced Fig. 1c from the monograph by Esau (1980, p. 467) for bean.

Figure 2a shows an early developmental stage. The outer and inner parenchymas separated by a network of vascular bundles are distinctly seen in the bean pod (1). The inner parenchyma is larger as compared with the outer one, earlier differentiated. The dorsal and ventral sutures contain strands of vascular bundles (3). The embryonic tissues (2) are differentiated. The embryonic axis and cotyledons are distinctly seen as well as lighter colored tissue encompassing cotyledons, which later gives multilayer seed coat with vascular bundles.

Changes in the seed coat with several formed layers are most pronounced (Fig. 2b; age, 17 days). The outer layer is considerably and homogeneously hydrated. The inner layer in tomograms looks dark; vascular bundles start to develop initially as separate nodes (Fig. 2b) and then (Fig. 2c; 24 days) as individual bundles. The seed increases in size.

At the same time, the vascular tissues of the embryonic axis differentiate; procambial strands appear inside cotyledons; and the vascular bundles covering the bean pod (9) become more distinct. Figures 2d–2f show a mature seed with the vascular bundles of seed coat (7) and bean pod (9) as well as the procambial strands (8) filling the cotyledons. The sections passing through the funiculus and hilum tissue (Fig. 2e) and the entrance of a large pod bundle below the hilum (11) (Fig. 2f) are also shown for this age (31 days).

Figure 3 shows the tomograms of longitudinal sections: 3a–3c, the first harvesting of seeds on day 10 after fertilization; the scale bar is shown in Fig. 3b. Figures 2d–2i are the tomograms of the seed harvested on day 31; longitudinal sections at different levels are shown. In Fig. 3a, the section passes through the bean pod; the vascular bundles in pod halves are very thin and form a hardly noticeable network; Fig. 3c shows the section passing approximately in the middle of the bean; the vascular bundles running along the pod sutures are seen. Figures 3d–3i show a mature seed with a developed vascular system; the vascular system of bean pod (1) is seen as light lines with a network structure in Fig. 3d. The vascular bundles of seed coat (3), running from the hilum line to the opposite bean side are shown in Fig. 3e. The procambial strands appear in cotyledons (4) in their outer part, as is seen in Fig. 3f. Figures 3g and 3h show the sections through the center of the seed, containing the embryonic axis and Fig. 3i shows the section in the third perpendicular plane, planar, passing through the embryonic axis.

The procambial tissues inside the cotyledons form branched stands running from the embryonic axis. Figure 3h shows the vascular tissue inside the embryonic axis (6) and funiculus (7) and a large vascular bundle below the hilum (8) as well as the vascular bundles running along the ventral suture (5).

The section in a planar projection (Fig. 3i) demonstrates a more distinct image of the vascular tissue in the region of the embryonic axis.

DISCUSSION

Seeds of leguminous plants are convenient model objects for studying the processes involved in seed growth and development, the fluxes of nutrients during ontogenesis, the factors controlling these fluxes, and the possibilities for producing more valuable foodstuff. This is why their structure and growth processes are still intensively studied.

Tissues and Vascular Bundles of Bean Pod Wall

Fruit walls are formed of the carpel folded long its main (central) vein and joined at the edges (Bailey and Swamy, 1951). The edge of the pod carrying ovaries is referred to as the ventral suture; it contains lateral (Esau, 1980) vascular cords. The ventral suture on the opposite side of the pod also has vascular cords (Reeve and Brown, 1968). In tomograms, they are seen as several strong parallel strands (Figs. 3g, 3h) (5). The pods are covered with a network of vascular bundles, resembling leaf venation; in morphology, seed bud is regarded as a modification of leaf structure (Aleksandrov, 1954).

All the vascular tissues of pod walls develop within a juvenile outer parenchyma during the floral and post-floral growth (Reeve and Brown, 1968). Vascular cords never develop in the inner parenchyma. As early as on day 10 after fertilization, the surface of pod walls (Fig. 3a) is covered with a network of small hardly noticeable bundles, which grow with the growth of the fruit (Fig. 3d, 1) and contain both phloem and xylem elements. Small veins can contain incomplete (only of phloem) vascular bundles (Yakovlev, 1991). Since the outer pod parenchyma contain chloroplasts, it can be involved in assimilation and conduct nutrients via the phloem elements of the pod to the lateral vascular cords in addition to the fluxes of assimilates from the leaves.

Tissues and Vascular Bundles of Seed Coat

It has been earlier considered that the seed coat of mature seeds plays only a protective function. So far, numerous studies have demonstrated that the legume seed coat is a multifunctional organ supplying nutrients to the embryo during seed development (Thorne, 1985; Murray, 1987; Zhang et al. 2007; etc.).

The architecture of the vascular bundles in the seed coat in the family Fabaceae is variable and can have a taxonometric value. In particular, the seed coat of soy-

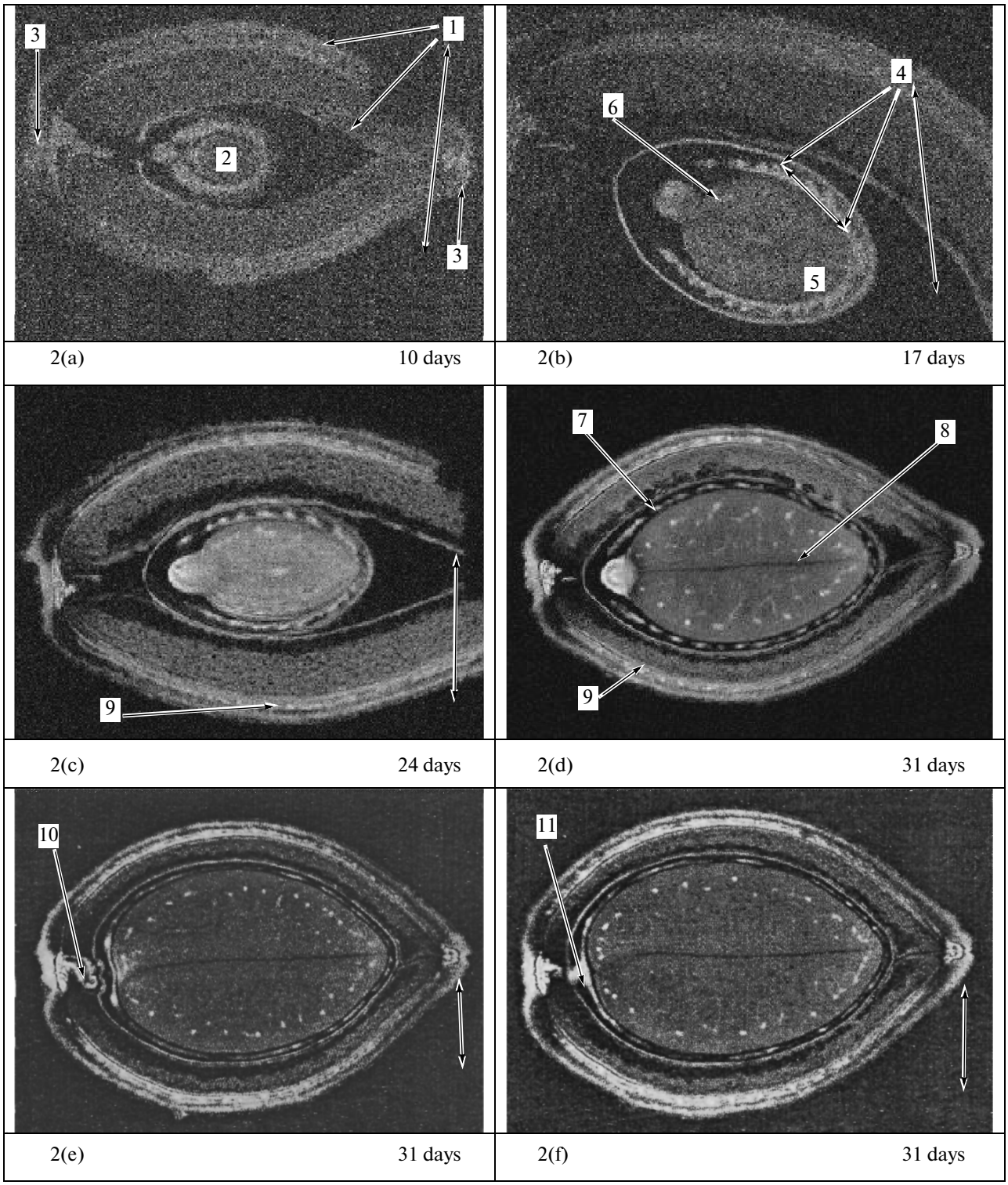

Fig. 2. Tomographic cross-sections of *Phaseolus limensis* beans at different developmental stages. The images are made at different magnifications; white scale arrows, 5 mm. The bean position in circuit corresponds to that shown in Fig. 1a. The tomograms were recorded by gradient echo technique using a 512 × 512 px image sensor and field of view of 1.5 cm for 2a and b, 2.5 cm for 2c, and 3.0 cm for the remaining images (2d)–(2f). Section thickness is 0.3 mm for 2a and 2b, 0.4 mm for 2c, and 0.7 mm for (2d)–(2f). Designations: (1) pod; (2) embryo; (3) vascular bundles in lateral pod sutures; (4) seed coat with vascular bundles; (5) cotyledons; (6) embryonic axis; vascular bundles of (7) seed coat, (8) cotyledons; (9) pod; and (10) funiculus tissue; and (11) large vascular bundle under the hilum. See text for details.

bean (*Glycine max*) and bean (*Phaseolus vulgaris*), which belong to the tribe Phaseoleae, have a branched network of vascular bundles versus the seed coat of pea (*Pisum sativum*) and broad beans (*Vicia faba*), belonging to the tribe Vicieae, which contain only one chalazal vein with two lateral branches (Van Dongen et al., 2003).

The seed coat is a genetically maternal organ; the embryo is a daughter organ. The seed coat is a mediator between the embryo and maternal plant. During the maturation stage, sucrose and other nutrients enter the seeds through the ventral vascular system, localized along the pod, to the region around the hilum; from the hilum, this system branches over the seed coat to the opposite side of the seed.

The structure of the bean seed coat has been repeatedly studied using light and electron microscopy. It has been demonstrated that the seed coat is formed of many layers. Its structure has been comprehensively described by Sterling (1954), Esau (1980), Zhou et al. (2007), etc. Figure 4a shows the image of a seed coat cross-section adopted from (Zhou, 2007). The outer layer is formed of macrosclereids. Below, the hourglass-shaped cells with large intercellular space are located. Under them, there are sclerenchyma, a loose tissue with large intercellular space, which is followed by ground parenchyma, the middle part of which contains vascular bundles. The ground parenchyma is followed by a layer of branched parenchyma; in soybean seeds, this part of the seed coat is referred to as aerenchyma (Thorne, 1981).

The seed coat tissues in tomograms differ in the intensity of water signal. The outer layer tissue with a strong signal from water can be ascribed to the seed coat part that contains macrosclereid, hourglass-shaped, and sclerenchyma cells. Its high degree of hydration is explainable by the fact that the vascular bundles from the placenta through funiculus pass near the hilum. This is well evident on the cross-sections shown in Fig. 2e. Several vascular bundles enter this layer, but they contact only the outer layer, which lacks vascular bundles. Since the structure of this layer is rather loose, nutrient solutions can occupy the free place there.

The dark seed coat regions in tomograms belong to parenchymatous tissues. The vascular bundles located there are connected with the lateral strands of the fruit via a large vascular bundle, the entrance of which is distinctly seen in both the tomographic cross-sections (Fig. 2f, *11*) and longitudinal (Fig. 3h, *8*) sections. This entrance is located between the hilum and lens. We first found it in the paper by Aniskin and Saprykina (1962), the corresponding figure from which is reproduced in Fig. 4c, and then observed it in the tomograms. Thus, two entrances of vascular bundles through the placenta and funiculus to the seed coat are seen in tomograms. The mentioned papers on the transport of assimilates into bean seeds consider only single bundle passing through the funiculus (for example, Fig. 4b)

A low degree of hydration in the seed coat parenchyma can be associated with destruction of its cells (Esau, 1980); filling of its cell envelopes with cork, cutin, lignin, etc., to provide stability (Tsinger, 1958); and obliteration (*Sravnitel'naya*..., 1996).

Our data on the architecture of vascular bundles in the *Phaseolus limensis* seed coat agrees well with the microscopy data for soybean (Thorne, 1981) that we show in Fig. 4d. Thorne has demonstrated that a large vascular bundle after entering the seed coat is connected with two other bundles almost perpendicular to it and enveloping the hilum tissues from both sides. Numerous smaller cords run on both sides from these two large cords in the seed coat inner parenchyma, repeatedly anastomosing within the parenchyma. From small cords, assimilates are unloaded into parenchymatous tissues. We have not found any vascular connection between the seed coat and cotyledons of the developing embryo by MRI.

Conductive System of the Embryo: Cotyledons and Embryonic Axis

The tomographic method allowed us to observe the development and architecture of embryonic conductive tissues in a noninvasive manner.

According to Aleksandrov (1954), normally differentiated embryos should have a well-developed conductive system, which passes through the center of root and stem buds and branches into the cotyledons. According to Tsinger (1958), this system is represented by procambial strands, which from the central cylinder of root run into the cotyledons and frequently anastomose there. The embryonic conductive system is a completely independent separated system without any connections with the conductive pathways of the maternal plant (Tsinger, 1958).

Obviously, the vascular tissues have a primitive structure and are represented by procambial strands. According to tomographic images, they permeate all the parts of the mature seed, being arranged as a circular zone in the radicle and hypocotyl, enter the budlet (Fig. 3h), and run down from the embryo to cotyledons, where they form a branched network, especially densely filling the outer parts of cotyledons (Fig. 3g). In the tomograms, we have not found any connections between them and the vascular bundles of the seed coat. Indeed, the conductive system of the embryo is independent and is established to commence functioning when seeds start to germinate. For example, histological studies have demonstrated the absence of any mature or differentiated vascular elements in the *Arabidopsis thaliana* embryo; its vascular system was represented by a continuous network of procambial cells in the radicle, hypocotyl, and cotyledons. After seed germination, procambium differentiates into xylem and phloem, which become distinguishable as

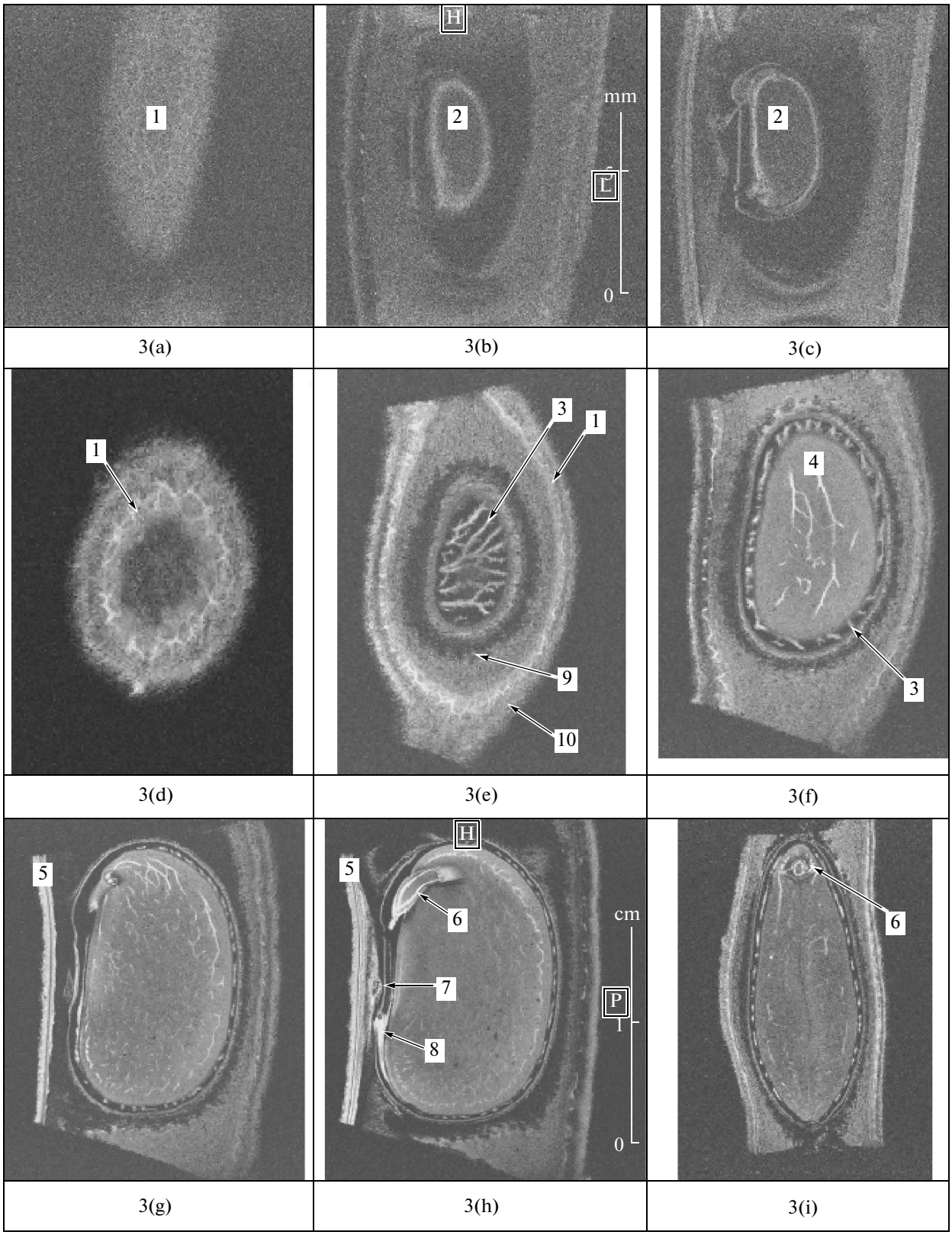

Fig. 3. Tomograms of longitudinal sections of *Phaseolus limensis* beans (3a)–(3c) on day 10 after fertilization and (3d)–(3i) on day 31. The bean position in circuit corresponds to that shown in Fig. 1a. The tomograms were recorded by gradient echo technique using a 512 × 512 px image sensor and field of view of 1.5 cm for (2a)–(2c) and to 3.0 cm for the remaining images (2d)–(2i). Section thickness is 0.3 mm. Designations: (1) pod with a network of vascular bundles; (2) embryo; vascular bundles of (3) seed coat, (4) cotyledons, (5) pod ventral suture, and (6) embryonic axis; (7) funiculus tissue; (8) large vascular bundle under the hilum; and (9) outer and (10) inner parenchymas separated by vascular bundles. See text for details.

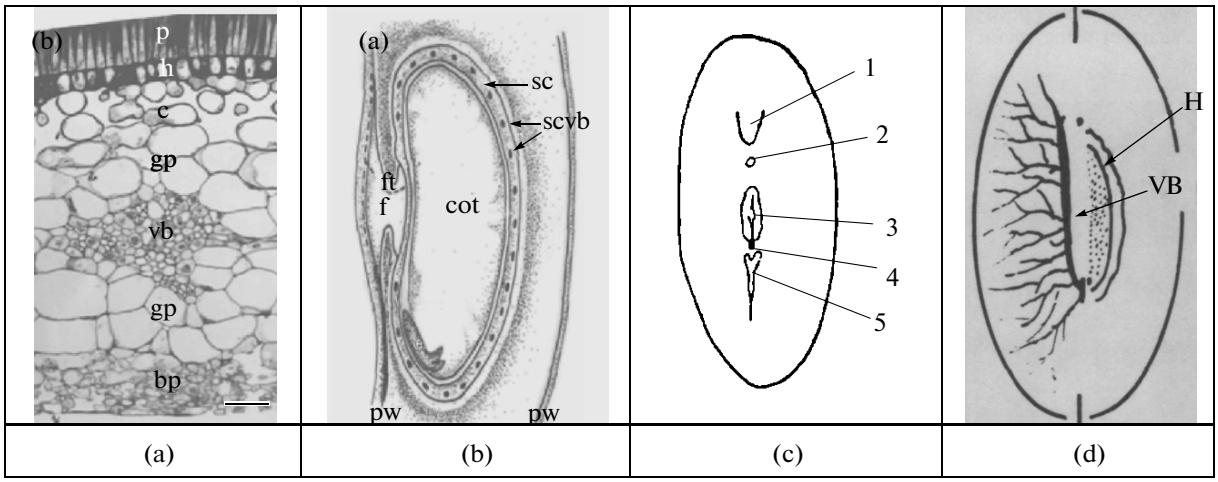

Fig. 4. (a) Cross-section of *Phaseolus limensis* seed coat (light microscopy): p—palisade cell layer; h—hypodermis; c—chlorenchyma; gp—ground parenchyma; bp—branched parenchyma; and vb—vascular bundles (reproduced from Zhou et al., 2007). (b) Scheme of the *Phaseolus vulgaris* seed in the pod with vascular bundles: pw—pod wall; f—funiculus; ft—funiculus trace; cot—cotyledon; sc—seed coat; and scvb—vascular bundles in the seed coat (reproduced from Zhou et al., 2007). (c) Scheme of the hilum region of the *Phaseolus seed*: (1) radicle; (2) micropile; (3) hilum cleft; (4) entrance site of vascular bundle; and (5) lens (reproduced from Aniskin and Saprykina, 1962). (d) Scheme of the vascular bundles of the soybean seed coat: H—hilum and VB—vascular bundles (reproduced from Thorne, 1981).

early as in 6-day-old seedlings (Busse and Evert, 1999).

Differentiated vascular elements have also been observed by MRI in the hypocotyl of 6-day-old castor oil plant seedlings (Verscht et al., 1998).

Pathways of Nutrient Supply to Bean Fruits and Seeds

This issue has been repeatedly studied and is still discussed. Currently, the model postulates that the substances necessary for development of embryo are assimilated in leaves and supplied to the bean pod and then through the funiculus to the seed coat and to its vascular bundles localized to the middle part of inner ground parenchyma. Since there are no direct connection between these channels and the embryo, the assimilates from the pod phloem elements are poured into the transfer cells of parenchyma, being discharged along the entire length of pod veins, and are transported over the symplast from the sieve elements to adjacent parenchymatous cells. Then they are radially transported inwards via a symplast route and accumulate near the seed via the apoplast through the intercellular space (Patrick and Offler, 2001).

During seed development, the seed coat should import the excess water. Taking into account the impermeability of the epidermal cuticle covering the seed coat, any evacuation of water from the seed should go through the funiculus and bean pod. Presumably, seeds return water to the pod vascular bundles through the pod xylem, funiculus, and veins of dorsal suture; otherwise the incoming phloem sap would dissolve. Within the seed coat, water should return through xylem (Pate et al., 1985; Peoples et al., 1985).

Thus, we have demonstrated the possibility to study the seed growth, development, and conductive system as well as to analyze the pathways for uptake of nutrients by noninvasive MRI technique. Not reaching the high-resolution characteristic of light and electron microscopy, MRI makes it possible to work with plant objects in the absence of artifacts associated with destruction of specimens.

ACKNOWLEDGMENTS

The work was supported by the targeted program "Development of the Research Potential of Higher School" (project no. 2.1.1/2584).

REFERENCES

Aleksandrov, V.G., *Anatomiya rastenii* (Anatomy of Plants), Moscow: Sovetskaya nauka, 1954.

Aniskin, V.I. and Saprykina, E.G., On Water Permeability of Seeds of Forage Legumes and Lupins, *Sel. Semenovod.*, 1962, no. 4, pp. 18–22.

Van As, H., Scheenen, T.W.J., and Vergeldt, F.J., MRI of Intact Plants, *Photosynth. Res.*, 2009, vol. 102, pp. 213–222.

Bailey, I.W. and Swamy, B.G.L., The Conduplicate Carpel of Dicotiledons and Its Initial Trends of Specification, *Am. J. Bot.*, 1951, vol. 38, pp. 373–379.

Blümich, B. and Kuhn, W., *Magnetic Resonance Microscopy: Methods and Application in Materials Science, Agriculture and Biomedicine,* New York: VCH Publishers. B, 1992.

Busse, J.S. and Evert, R.F., Pattern of Differentiation of the First Vascular Elements in the Embryo and Seedling of *Arabidopsis thaliana*, *Int. J. Plant Sci.*, 1999, vol. 160, pp. 1–13.

Callaghan, P.T., *Principles of Nuclear Magnetic Resonance Microscopy*, Oxford: Oxford Univ. Press, 1991.

Chudek, J.A. and Hunter, G., Magnetic Resonance Imaging of Plants, *Progr. Nucl. Mag. Res. Sp.*, 1997, vol. 31, pp. 43–62.

Ciobanu, L., Webb, A.G., and Pennington, C.H., Magnetic Resonance Imaging of Biological Cells, *Progr. Nucl. Mag. Res. Sp.*, 2003, vol. 42, pp. 69–93.

Connelly, A., Lohman, J.A.B., Loughman, B.C., et al., High Resolution Imaging of Plant Tissue by NMR, *J. Exp. Bot.*, 1987, vol. 38, pp. 1713–1723.

Van Dongen, J.T., Ammerlaan, A.M.H., Wouterlood, M., et al., Structure of the Developing Pea Seed Coat and the Post-Phloem Transport Pathway of Nutrients, *Ann. Bot.*, 2003, vol. 91, pp. 729–737.

Esau, K., *Anatomiya semennykh rastenii* (Anatomy of Seed Plants), Book 2, Moscow: Mir, 1980.

Farrar, T.C. and Becker, E.D., *Pulse and Fourier Transform NMR: Introduction to Theory and Methods,* New York: Academic Press. B, 1971.

Fiziologiya sel'skokhozyaistvennykh rastenii (Physiology of Crop Plants), Vol. 6: *Zernobobovye rasteniya. Mnogoletnie travy. Khlebnye zlaki* (Leguminous Plants. Perennial Grasses. Crop Plants), Turkov, N.S., Ed., Moscow: Mosk. Gos. Univ., 1970.

Foster, M.P. and Hutchinson, J.M.S., *Practical NMR Imaging*, Oxford: IRL Press. B, 1987.

Garnczarska, M., Zalewski, T., and Kempka, M., Water Uptake and Distribution in Germinating Lupine Seeds Studied by Magnetic Resonance Imaging and NMR Spectroscopy, *Physiologia Plantarum*, 2007, vol. 130, pp. 23–32.

Garnczarska, M., Zalewski, T., and Wojtyla, L., A Comparative Study of Water Distribution and Dehydrin Protein Localization in Maturing Pea Seeds, *J. Plant Physiol.*, 2008, vol. 165, pp. 1940–1946.

Glidewell, S.M., Williamson, B., Goodman, B.A., et al., An NMR Microscopic Study of Grape (*Vitis vinifera* L.), *Protoplasma,* 1997, vol. 198, pp. 27–35.

Glidewell, S.M., NMR Imaging of Developing Barley Grains, *J. Cereal Sci.*, 2006, vol. 43, pp. 70–78.

Goodman, B.A., Williamson, B., and Chudek, J.A., Nuclear Magnetic Resonance (NMR) Micro-Imaging of Raspberry Fruit: Further Studies on the Origin of the Image, *New Phytol.*, 1992, vol. 122, pp. 529–535.

Gyngell, M.L., The Application of Steady-State Free Precession in Rapid 2DFT NMR Imaging: FAST and CE-FAST Sequences, *Magn. Res. Imag.*, 1988, vol. 6, pp. 415–419.

Hausser, K.H. and Kalbitzer, H.R., *NMR in Medicine and Biology: Structure Determination, Tomography, in vivo Spectroscopy*, Berlin: Springer-Verlag, 1991.

Horigane, A.K., Takahashi, H., Maruyama, S., et al., Water Penetration into Rice Grains during Soaking Observed by Gradient Echo Magnetic Resonance Imaging, *J. Cereal Sci.,* 2006, vol. 44, pp. 307–316.

Ishida, N., Koizumi, M., and Kano, H., The NMR Microscope: A Unique and Promising Tool for Plant Science, *Ann. Bot.*, 2000, vol. 86, pp. 259–278.

Ishida, N., Naito, S., and Kano, H., Loss of Moisture from Harvested Rice Seeds on MRI, *Magn. Res. Imag.*, 2004, vol. 22, pp. 871–875.

Köckenberger, W., Pope, J.M., Xia, Y., et al., A Non-Invasive Measurement of Phloem and Xylem Water Flow in Castor Bean Seedlings by Nuclear Magnetic Resonance Microimaging, *Planta*, 1997, vol. 201, pp. 53–63.

Köckenberger, W., Functional Imaging of Plants by Magnetic Resonance Experiments, *Trends Plant Sci.*, 2001, vol. 6, no. 7, pp. 286–292.

Köckenberger, W., De Panfilis, C., Santoro, D., et al., High Resolution NMR Microscopy of Plants and Fungi, *J. Microsc.*, 2004, vol. 214, pp. 182–189.

Kikuchi, K., Koizumi, M., Ishida, N., et al., Water Uptake by Dry Beans Observed by Micro-Magnetic Resonance Imaging, *Ann. Bot.*, 2006, vol. 98, pp. 545–553.

Koptyug, I.V. and Sagdeev, R.Z., Modern Physicochemical Applications of NMR Tomography. The Specificity of the Method and Its Application to the Study of Liquid-Containing Objects, *Usp. Khim.*, 2002, vol. 71, no. 7, pp. 672–699.

Lauterbur, P.C., Image Formation by Induced Local Interactions: Examples Employing Nuclear Magnetic Resonance, *Nature,* 1973, vol. 242, pp. 190–191.

MacFall, J.S. and Johnson, G.A., The Architecture of Plant Vasculature and Transport as Seen with Magnetic Resonance Microscopy, *Can. J. Bot.*, 1994, vol. 72, pp. 1561–1573.

Manz, B., Muller, K., Kucera, B., et al., Water Uptake and Distribution in Germinating Tobacco Seeds Investigated in vivo by Nuclear Magnetic Resonance Imaging, *Plant Physiol.,* 2005, vol. 138, pp. 1538–1551.

Morris, P.G., *Nuclear Magnetic Resonance Imaging in Medicine and Biology*, Oxford: Clarendon Press, 1986.

Murray, D.R., Nutritive Role of Seed Coats in Developing Legume Seeds, *Am. J. Bot.*, 1987, vol. 74, pp. 1122–1137.

Öpik H., Development of Cotyledon cell Structure in Ripening *Phaseolus vulgaris* Seeds, *J. Exp. Bot.*, 1968, vol. 19, no. 58, pp. 64–76.

Pate, J.S., Kuo, J., Van Bel, A.J.E., et al., Diurnal Water Balance of the Cowpea Fruit, *Plant Physiol.*, 1985, vol. 77, pp. 148–156.

Patrick, J.W. and Offler, C.E., Compartmentation of Transport and Transfer Events in Developing Seeds, *J. Exp. Bot.*, 2001, vol. 52, pp. 551–564.

Peoples, M.B., Pate, J.S., Atkins, C.A., et al., Economy of Water, Carbon and Nitrogen in the Developing Cowpea Fruit, *Plant Physiol.*, 1985, vol. 77, pp. 142–147.

Pfeffer, P.E. and Gerasimowicz, W.V., *Nuclear Magnetic Resonance in Agriculture*, Boca Raton.: CRC Press, 1989.

Pietrzak, L.N., Fregeau-reid, J., Chatson, B., et al., Observation on Water Distribution in Soybean Seed during Hydration Processes Using Nuclear Magnetic Resonance Imaging, *Can. J. Plant Sci.*, 2002, vol. 82, pp. 513–519.

Reeve, R.M. and Brown, M.S., Histological Development of the Green Bean Pod as Related to Culinary Texture.

1. Early Stages of Pod Development, *J. Food Sci.*, 1968, vol. 33 P, pp. 321–326.

Rinki, P.A., *Magnitnyi rezonans v meditsine* (Magnetic Resonance in Medicine), Moscow: Geotar-Med, 2003.

Scheenen, T.W.J., Van Dusschoten, D., de Jager, P.A., et al., Quantification of Water Transport in Plants with NMR Imaging, *J. Exp. Bot.*, 2000, vol. 51, pp. 1751–1759.

Scheenen, T.W.J., Vergeldt, F.J., Heemskerk, A.M., et al., Intact Plant Magnetic Resonance Imaging to Study Dynamics in Long-Distance Sap Flow-Conducting Surface Area, *Plant Physiol.*, 2007, vol. 144, pp. 1157–1165.

Sterling, C., Development of the Seed Coat of Lima Bean (*Phaseolus lunatus* L.), *Bull. Torrey Bot. Club,* 1954, vol. 81, no. 4, pp. 271–287.

Thorne, J.H., Phloem Unloading of C and N Assimilates in Developing Seeds, *Ann. Rev. Plant Physiol.*, 1985, vol. 36, pp. 317–343.

Tsinger, N.V., *Semya, ego razvitie i fiziologicheskie svoistva* (Seed, Its Development and Physiological Properties), Moscow: Akad. Nauk SSSR, 1958.

Verscht, J., Kalusche, B., Köhler, J., et al., The Kinetics of Sucrose Concentration in the Phloem of Individual Vascular Bundles of the *Ricinus communis* Seedling Measured by Nuclear Magnetic Resonance Microimaging, *Planta*, 1998, vol. 205, pp. 132–139.

Vinogradova, I.S. and Falaleev, O.V., Application of Magnetic Resonance Microtomography for Studying the Internal Structure of Plants, *Sel'skokhoz. Biol.*, 2010a, no. 3, pp. 118–124.

Vinogradova, I.S. and Falaleev, O.V., Application of Magnetic Resonance Microtomography for Studying the Internal Structure of Legume Seeds, *Vestnik Ross. Akad. Sel'skokhoz. Nauk*, 2010b, no. 6, pp. 10–12.

Weber, H., Borisjuk, L., and Wobus, U., Molecular Physiology of Legume Seed Development, *Annu. Rev. Plant Biol.*, 2005, vol. 56, pp. 253–279.

Williamson, B., Goodman, B.A., Chudek, J.A., et al., The Vascular Architecture of the Fruit Receptacle of Red Raspberry Determined by 3D NMR Microscopy and Surface-Rendering Techniques, *New Phytol.*, 1994, vol. 128, pp. 39–44.

Xia, Y., Sarafis, V., Campbell, E.O., et al., Non Invasive Imaging of Water Flow in Plants by NMR Microscopy, *Protoplasma*, 1993, vol. 173, pp. 170–176.

Yakovlev, G.P., *Bobovye zemnogo shara* (Legumes of the World), Leningrad: Nauka, Leningr. Otd., 1991.

Zhang, W.H., Zhou, Y., Dibley, K.E., et al., Nutrient Loading in Developing Seeds, *Funct. Plant Biol.*, 2007, vol. 34, pp. 314–331.

Zhou, Y., Setz, N., Niemietz, C., et al., Aquaporins and Unloading of Phloem-Imported Water in Coats of Developing Bean Seeds, *Plant, Cell Environ.*, 2007, vol. 30, pp. 1566–1577.